

CHAPTER 2

Experimental Section:

2.0 Introduction:

This chapter describes the details of the experimental setup and explains the principles of the techniques used in study.

2.1 Electrochemical cell:

The electrochemical cell is made of glass with a teflon lid machined to fit with the B-55 size neck. The teflon lid accommodates the working, reference and counter electrodes. There is also a provision for gas inlet and outlet for deaerating the cell. All the electrodes are fitted with a ground joint of size B-14 to insert into the cell. The counter electrode is a platinum strip which is sealed to a glass tube. The working electrode is held by an electrode holder as shown in figure. The working electrode holder is a gold plated brass rod with a slot at one end in which the working electrode is held with the help of screws. This holder is fixed to a teflon B-14 cone which is fixed to the socket of the central ground joint. The reference electrode has a luggin capillary which can be positioned near the working electrode to minimise the IR drop. For studies in ethanol the reference electrode is kept in a separate compartment connected through a glass tube with a stop cork so as to prevent mixing.

2.2 Preparation of working electrode:

In this section, surface pretreatments for the polycrystalline samples are described. We have carried out studies on the effect of the following surface treatments: Mechanical polishing, Chemical etching, Electropolishing.

2.2.1 Mechanical polishing:

The working electrodes used were copper, silver and gold. All of them were >99.9% pure. Araldite was applied on the electrode so as to mask all the other regions of the electrode except a well defined and known surface area. Parafilm (a fluoropolymer) and teflon tape were wrapped over the araldite layer to prevent any chemical attack on the resin. The electrodes were hand polished with emery papers of grade 800,1000,1500 whose particle sizes are 17 μm , 13 μm and 9 μm respectively depending on the roughness required. Alumina treated specimens were prepared by first polishing them with emery, followed by polishing successively on a microcloth having a slurry of 1,0.3,0.05 μm alumina powder (Buehler). The electrode was ultrasonically cleaned in distilled water to remove alumina particles. It was finally cleaned with millipore water.

2.2.2 Chemical etching:

All the electrodes were polished with alumina powder prior to etching. After sonication in distilled water chemically etched surfaces of copper and silver were prepared by dipping in concentrated nitric acid (8N) solution for one minute. Gold etching was done with aqua regia solution (3:1 HCl and HNO₃). After etching the electrodes were washed with milli pore water before introducing into the cell.

2.2.3 Electropolishing:

Copper electrode was electropolished in a solution containing 35 ml phosphoric acid (stock solution) and 9 ml of n-butanol. Stainless steel was used as the cathode. The current density was maintained at 1.5 A cm⁻² for one minute. Gold electropolishing [1] was done in a solution containing 4 gm dm⁻³ KCN and 7 gm dm⁻³ of potassium sodium tartarate. The current density was maintained at 1 Acm⁻² for one minute.

2.3 Preparation of Au (111) surface:

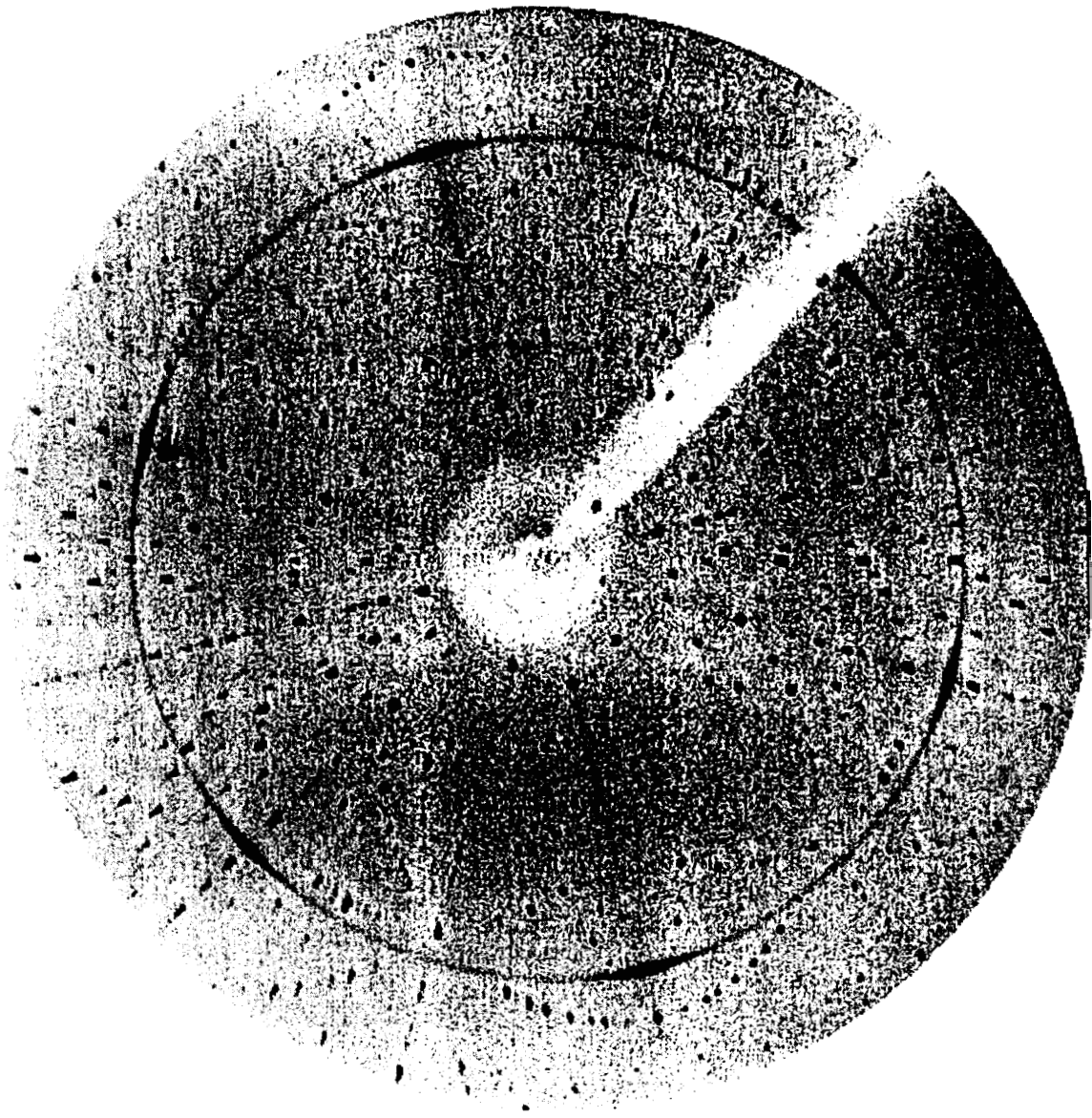
Au (111) surface was prepared by evaporation of gold onto Muscovite mica [2,3]. The mica surface was cleaved just before mounting into the vacuum chamber (Hindhivac). The mica substrate after mounting into the vacuum chamber was cleaned by ion bombardment using oxygen gas. The substrate temperature was maintained at 350⁰C throughout. The pressure in the vacuum chamber was 2×10⁻⁵ mbar. Resistive evaporation of gold was carried out at a rate of 4-5 Å⁰sec⁻¹. The substrate holder was rotated during evaporation in order to facilitate uniform deposition of gold over mica. The thickness of the gold film was monitored *in situ* using a quartz crystal microbalance. The final thickness of the gold film was 1020 Å. X-ray diffraction studies of the gold film confirmed that the crystallographic orientation is almost completely (111) in nature.

2.4 Pretreatment of the electrochemical cell:

The electrochemical cell was washed with soap powder and thoroughly flushed with free flowing water. It was then immersed in chromic acid solution and finally washed with distilled water. The cell and other glass ware used were kept in a hot air oven to be dried. This procedure was followed before each experiment.

2.5 Deaeration of solution with Nitrogen gas:

Whenever experiments are needed to be carried out with deaerated solution, nitrogen gas is passed through the solution. During the measurement, the gas is not bubbled into the solution but passed over it so that a nitrogen atmosphere is maintained over the solution inside the cell during the measurement.



X-Ray Diffraction pattern of evaporated gold on Mica showing predominantly Au(111) crystallographic orientation.

2.6 Experimental techniques:

The different experimental techniques used in the study of adsorption of azoles and alkanethiols onto gold, silver and copper are described below:

2.7 Cyclic voltammetry:

Cyclic voltammetry [4,5] consists of sweeping the potential of the working electrode between potential limits E_1 and E_2 at a known sweep rate v and then reversing the sweep. This results in the occurrence of oxidation or reduction reactions of electroactive species in the solution (faradic reaction) and a capacitive current due to double layer charging. The cell current is recorded as a function of applied potential. The sweep rates used in conventional experiments range from a few mV per sec upto a few hundred Volts per second.

Cyclic voltammetry is one of the most widely used techniques to study electrode processes. Kinetic parameters can be determined for a wide variety of mechanisms. An electrochemical spectrum indicating the potentials at which processes occur can be rapidly obtained while from the sweep rate dependence the involvement of coupled homogeneous reactions can be readily identified, and other processes such as adsorption can be recognised. Voltammograms can be recorded over a wide range of sweep rates and for various values of E_1 and E_2 . Usually there will be several peaks, and by observing how these peaks appear and disappear as the potential limits and sweep rates are varied, and also by noting the difference between the first and subsequent cycles it is possible to determine how the processes represented by the peaks are related. The difference between the first and subsequent cyclic voltammograms provides useful mechanistic information. The shape of the current–voltage curve in a cyclic voltammogram can be understood in the following way. On reaching a potential where the electrode reaction begins, the current rises. However the creation of a concentration gradient and consumption of electroactive species means that, continuing to sweep the

potential, from a certain value just before the maximum value of current, the peak current the supply of electroactive species begins to fall. Owing to the depletion of electroactive species the current begins to decrease. Overall this behaviour gives rise to a peak shaped potential-current response. Using similar arguments as were used in the forward sweep, it can be shown that the current on the reverse sweep will also exhibit a peaked response though of the opposite sign.

The important parameters in the input potential sweep are; the initial potential E_1 , the initial sweep direction, the sweep rate v , the maximum potential E_{\max} , the minimum potential E_{\min} and the final potential E_2 .

The peak current I_p of the cyclic voltammogram is given by the following relationship.

$$I_p = -0.4463nF \left(\frac{nF}{RT} \right)^{1/2} c_o^\infty D^{1/2} v^{1/2}$$

where,

I_p is the peak current density in $A cm^{-2}$,

D is the diffusion coefficient in $cm^2 sec^{-1}$

v is the sweep rate in $V sec^{-1}$

n is the number of electrons involved in the reaction

F is Faraday constant

R is gas constant

T is the absolute temperature.

This equation is called as the Randles- Sevcik equation .At $25^0 C$ the equation reduces to the form,

$$I_p = -(2.69 \times 10^5) n^{3/2} c_o^\infty D^{1/2} v^{1/2}$$

Thus we can see that the peak current density is proportional to the concentration of the electroactive species and to the square roots of the sweep rate

and diffusion coefficient. The current is negative because it is the current for cathodic reaction.

A test of the reversibility of the system is to check whether a plot of I_p as a function of $\nu^{1/2}$ is both linear and passes through the origin.[or alternatively $(I_p/\nu^{1/2})$ is constant].If this is found to be true then further diagnostic tests can be applied all of which should be satisfied by a reversible system. For a reversible system:

a) $\Delta E_p = |E_p^A - E_p^C| = \frac{59}{n} \text{ mV}$

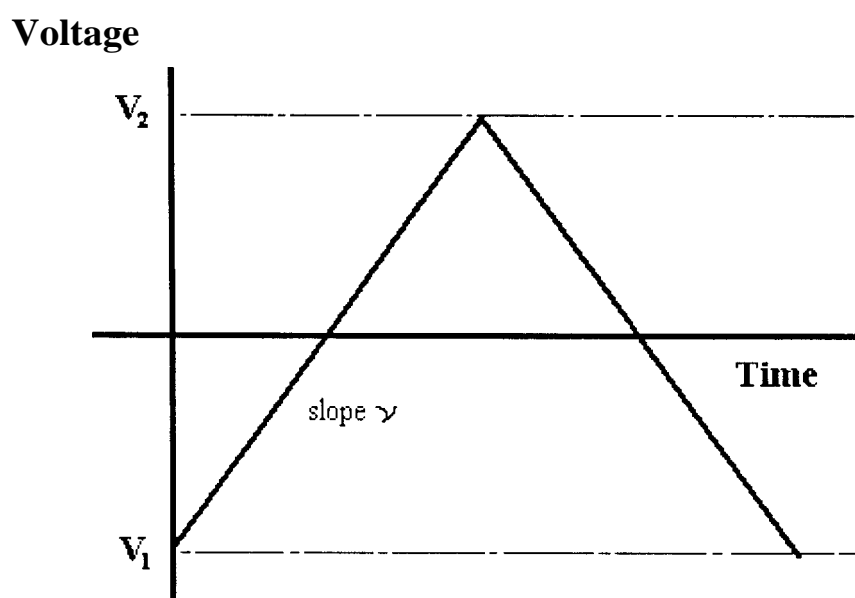
b) $|E_p - E_{p/2}| = \frac{59}{n} \text{ mV}$

c) $\left| \frac{I_p^A}{I_p^C} \right| = 1$

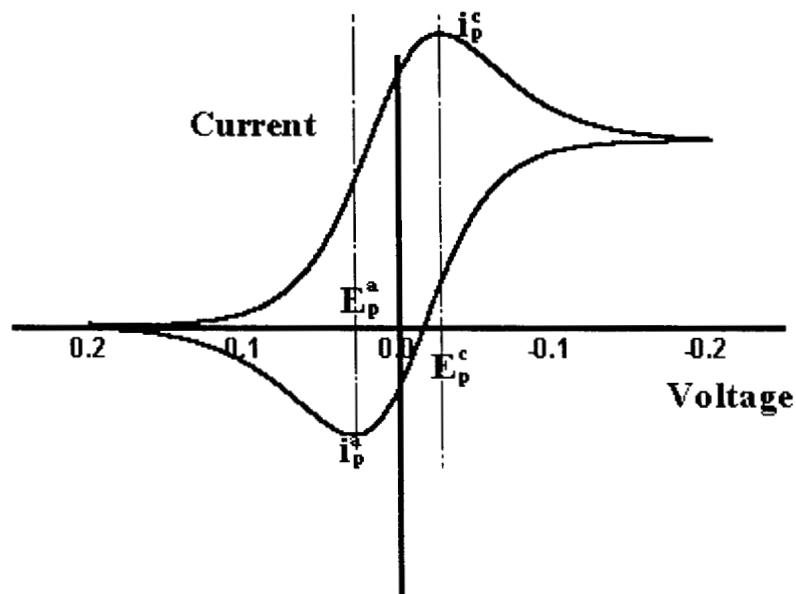
d) $I_p \propto \nu^{1/2}$

e) E_p is independent of ν .

f) At potentials beyond E_p , $I^{-2} \propto t$.



Potential – time profile for cyclic voltammetry



Cyclic voltammogram for a reversible process

2.7.1 Measurement of real surface area by adsorption/stripping from solution using cyclic voltammetry:

The method based on hydrogen adsorption [6] from solution is used to determine the real surface area for metals which show hydrogen adsorption in potential regions prior to massive H_2 gas evolution. This method has been established mainly with Pt electrodes but it has been extended to Rhodium and Iridium electrodes also.

The charge under the voltammetric peaks for hydrogen adsorption or desorption, corrected for double layer charging (the capacitive current), is assumed to correspond to the adsorption of one hydrogen atom on each metal atom on the surface (1,1). The charge associated with a one to one H-M correspondence per unit surface area Q_{11}^S is calculated on the basis of the distribution of the metal atoms at the surface. In the case of polycrystalline platinum the accepted value is $210 \mu C$

cm^{-2} , based on the assumption that the density of atoms on such a surface is $1.31 \times 10^{15} \text{ cm}^{-2}$. The true surface area is given by,

$$\text{True surface area} = \frac{Q_H}{Q_H^0}$$

The method based on oxygen adsorption [6] is applicable to metals showing well developed regions for oxide monolayer formation and reduction. This method can be applied to gold. Oxygen is assumed to be chemisorbed in a monoatomic layer prior to oxygen evolution with a one to one correspondence with the surface metal atoms. This implies that the charge associated with the formation or reduction of the layer is,

$$Q_0 = 2 e N_A \Gamma_0 A$$

where ,

N_A is Avogadro's number

Γ_0 is the surface concentration of atomic oxygen ,assumed to be equal to

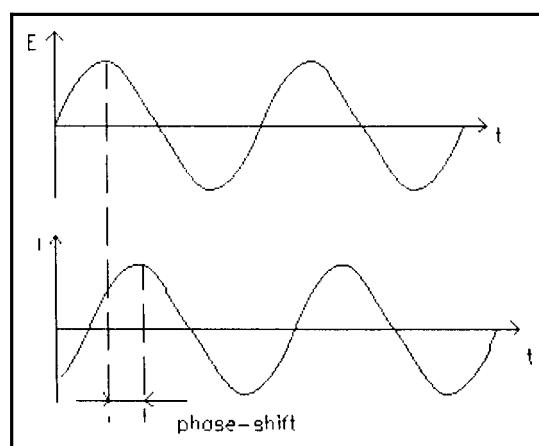
N_M the surface density of metal atoms.

From the value of N_M per unit area the value of Q_0 , the reference charge can be calculated. For polycrystalline gold this value is $400 \mu\text{C cm}^{-2}$. The roughness factor is calculated by dividing the charge obtained for monolayer formation for gold electrode per unit area by $400 \mu\text{C cm}^{-2}$.

$$\text{Roughness factor} = \text{True surface area} / \text{Geometric area}$$

2.8 Electrochemical Impedance Spectroscopy:

Electrochemical systems can be studied with methods based on impedance measurements [4,5,7]. These methods involve the application of a small perturbation, whereas in cyclic voltammetry the system is perturbed far from equilibrium. This small imposed perturbation can be of applied potential. The response to the applied perturbation which is generally sinusoidal can in general differ in phase and amplitude from the applied signal. Measurement of the phase difference and amplitude (i.e. impedance) permits analysis of electrode processes in relation to contributions from diffusion, kinetics, double layer, coupled homogeneous reactions etc. Impedance spectroscopy is extensively used in the study of corrosion, membranes, ionic solids, solid electrolytes etc.



Sinusoidal Current Response in a Linear System

The advantage of small perturbation lies in the ability to treat the response theoretically by linearised current-potential characteristics. Since one usually works close to equilibrium, the detailed knowledge about the behaviour of current-voltage response over great range of overpotential is not required. This advantage leads to important simplifications in treating kinetics and diffusion. Also high

precision measurements can be made because the response may be indefinitely steady and therefore can be averaged over a long term.

A comparison is usually made between the electrochemical cell and an equivalent electrical circuit that contains combinations of resistances and capacitances that are thought to behave like the cell. The aim of impedance measurement is to interpret these equivalent resistance and capacitance values in terms of interfacial phenomena. Impedance technique is capable of very high precision and is frequently used for the evaluation of heterogeneous charge transfer parameters and for studies of double layer structure.

2.8.1 Principles of A.C circuits:

The electrochemical response to an ac perturbation can be understood by knowing the fundamental principles of AC circuits. If a sinusoidal voltage $V = V_0 \sin \omega t$ where V_0 is the maximum amplitude and ω is the frequency is applied to an electrical circuit that contains a combination of resistors and capacitors, the response is a current given by,

$$I = I_0 \sin(\omega t + \phi)$$

where ϕ is the phase angle between the perturbation and response. The proportionality factor between V and I is the impedance Z .

In phasor terms the rotating vectors are separated on the polar diagram by the angle ϕ .

In case of a pure resistance R , Ohm's law $V = IR$ leads to,

$$I = \frac{V_0}{R} \sin \omega t$$

ϕ is zero. There is no phase difference between the potential and current

For a pure capacitor,

$$I = C \frac{dV}{dt}$$

Substituting one obtains,

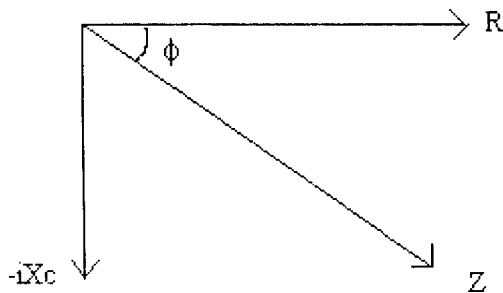
$$I = \omega C V_0 \sin\left(\omega t + \frac{\pi}{2}\right)$$

$$I = \frac{V_0}{X_C} \sin\left(\omega t + \frac{\pi}{2}\right)$$

Here we find that the phase angle is $\frac{\pi}{2}$, that is the current leads the potential by $\frac{\pi}{2}$.

$X_C = (\omega C)^{-1}$ is known as capacitive reactance.

The phase angles of resistances and reactances can be represented in two dimensions. On the x-axis the phase angle is zero; on rotating anti-clockwise about the origin the phase angle increases. Pure reactances are represented on the y-axis. The distance from the origin corresponds to the amplitude.



Representation in the complex plane of an impedance containing resistive and capacitive components

2.8.2 Equivalent circuit of an Electrochemical cell:

In a general sense, an electrode-solution interface is simply an impedance to a small sinusoidal excitation. The impedance $Z(\omega)$ of the electrochemical interface is a complex number which can be expressed in either polar coordinates or in Cartesian coordinates.

$$Z(\omega) = |Z| e^{j\phi}$$

$$|Z|^2 = (\text{Re } Z)^2 + (\text{Im } Z)^2$$

where $\text{Re } Z$ and $\text{Im } Z$ are the real part and the imaginary part of the impedance. The relationships between these quantities are:

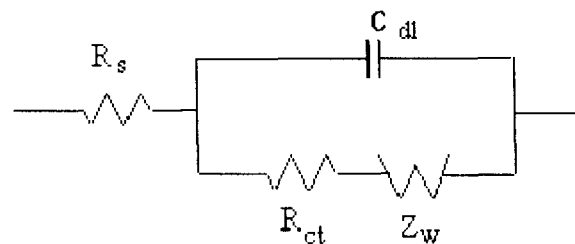
$$|Z|^2 = (\text{Re } Z)^2 + (\text{Im } Z)^2$$

$$\phi = \text{Arc tan } \frac{\text{Im } Z}{\text{Re } Z}$$

$$\text{Re}(Z) = |Z| \cos \phi$$

$$\text{Im}(Z) = |Z| \sin \phi$$

Hence its performance can be represented by an equivalent circuit of resistors and capacitors that pass current with the same amplitude and phase angle under a given excitation. A typical circuit is shown in the following figure.



Randles equivalent circuit for an electrode reaction with double layer capacitance C_{dl} , Warburg impedance Z_w and solution resistance R_s

The parallel elements are introduced because the total current through the working electrode is the sum of distinct contributions from the faradic process i_f and double layer charging i_c . The double layer capacitance exists at the interface between an electrode and its surrounding electrolyte. Charges in the electrode are separated from the charges of the ions. The double layer capacitance closely resembles a pure capacitance; hence it is represented in the equivalent circuit by the element C_{dl} . The faradic impedance can be separated into the charge transfer resistance R_{ct} and the Warburg impedance Z_w which represents a kind of resistance to mass transfer because of diffusion. This impedance depends on the frequency of the potential perturbation. At high frequencies the Warburg impedance is small since diffusing reactants do not have to move very far. At low frequencies the reactants have to diffuse farther, thereby increasing the Warburg impedance. R_s is the uncompensated solution resistance between the working electrode and reference electrode. Since all the current must pass through the uncompensated resistance, R_s is inserted as a series element to represent this effect in the equivalent circuit. In contrast to R_s and C_{dl} , which are nearly ideal circuit elements, the components of faradic impedance are not ideal because they change with frequency ω .

For a planar diffusion field R_{ct} can be expressed as,

$$R_{ct} = \frac{RT}{nFI_0}$$

where I_0 is the exchange current.

The solution resistance R_s is given by the expression,

$$R_s = \frac{x}{\kappa A}$$

where,

x is the distance of the capillary tip from the electrode

A is the electrode area

κ is the solution conductivity.

The relative size of R_{ct} and Z_w at any given frequency is a measure of the balance between kinetic and diffusion control. If the exchange current density i_0 is very large, R_{ct} will tend to zero and will be too small to measure so that only Warburg impedance will be observed. On the other hand a very sluggish electrochemical reaction will have a high value of R_{ct} which will be the dominant term. A full analysis of the Randles equivalent circuit has two limiting cases. At low frequencies as $\omega \rightarrow 0$ the real and imaginary parts of impedance are found to be:

$$Z' = R_s + R_{ct} + \sigma \omega^{-1/2}$$

$$Z'' = \sigma \omega^{-1/2} + 2\sigma^2 C_{dl}$$

$$\text{where, } \sigma = \frac{RT}{\sqrt{2}n^2 F^2 AD^{1/2}} \left(\frac{1}{c_0^x} + \frac{1}{c_R^x} \right)$$

D is the diffusion coefficient for the species in the solution

A area of the electrode

c_0^x and c_R^x are the bulk concentrations of the oxidised and reduced species.

from which,

$$Z'' = Z' - R_s - R_{ct} + 2\sigma^2 C_{dl}$$

This is the equation of a straight line of unit slope and with an intercept on the real Z' axis of,

$$R_s + R_{ct} - 2\sigma^2 C_{dl}$$

At high frequencies where the Warburg impedance is negligible in relation to R_{ct} the two components are:

$$Z' = R_s + \frac{R_{ct}}{1 + \omega^2 C_{dl}^2 R_{ct}^2}$$

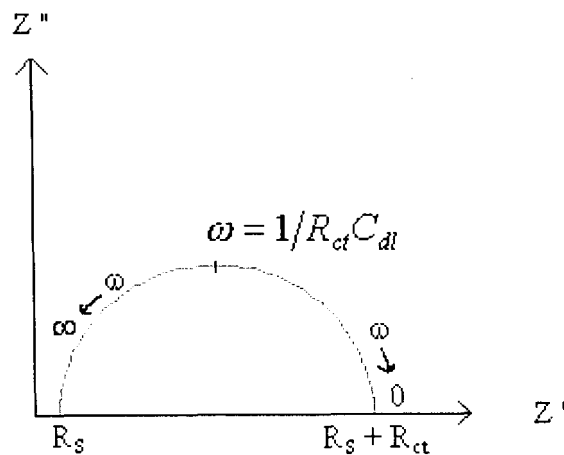
$$Z'' = \frac{C_{dl} R_{ct}^2 \omega}{1 + \omega^2 R_{ct}^2 C_{dl}^2}$$

Eliminating ω gives

$$(Z' - R_s - R_{ct}/2)^2 + (Z'')^2 = (R_{ct}/2)^2$$

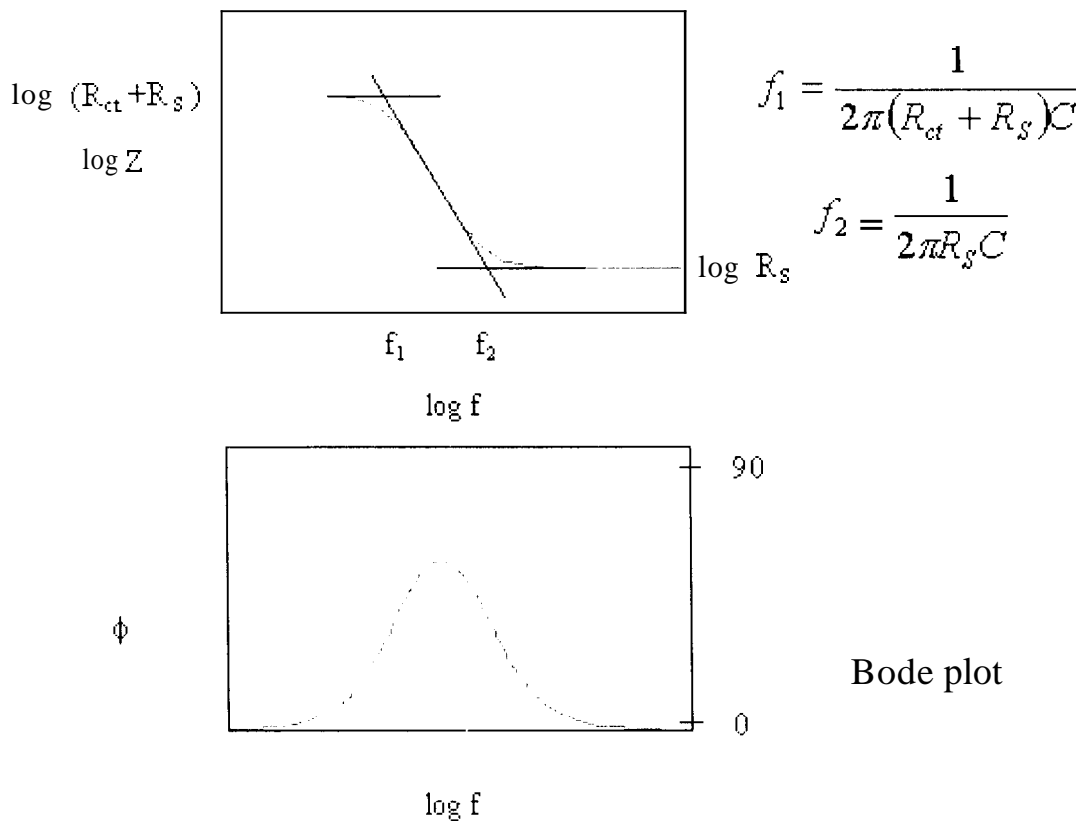
which is the equation of a circle centered on $Z' = R_s + R_{ct}/2$ with a radius of $R_{ct}/2$.

A plot of the whole expression for Z'' versus Z' for kinetic controlled reaction has the following form (Cole-Cole plot).



Cole-Cole plot

This plots Z' and Z'' at different frequencies. At infinite frequency Z'' approaches zero as the capacitance in the equivalent circuit offers very little impedance. At low frequencies the impedance is purely resistive, because the reactance of C is very large. The solution resistance has the effect of translating the semi circle on the Z' axis. R_s can be found by reading the real axis value at the high frequency intercept. C_{dl} is obtainable from the maximum value of Z'' in the semi circular region where $\omega = 1/R_{ct}C_{dl}$. The diameter of the semi circle is given by R_{ct} . Another way of presenting impedance data is by the Bode plot [8]. In this, logarithm of the modulus of impedance ($\log|Z|$) and the phase angle ϕ are both plotted in the y-axis with a common abscissa of log of frequency. On such a plot a pure resistance is represented by a horizontal line and a constant ϕ of 0° , while a pure capacitor is a straight line of slope -1 and a constant ϕ of -90° . The Bode plot for Randles equivalent circuit (without Warburg impedance) is shown in the figure.



The rounded transition between the horizontal and sloping section is called a corner and the frequency of the intersection of lines extrapolating the straight sections is called the corner frequency. The transitions between asymptotic values mark those frequency regions where the ohmic and capacitive components have comparable values, with neither one completely predominant. Presenting the impedance values in Bode plot is advantageous for those systems which have several time constants.

2.8.3 Measurement of impedance:

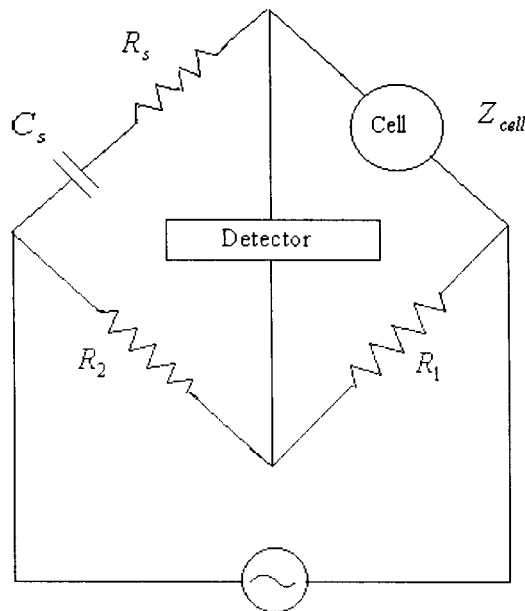
Due to the high frequency capacitive effect attributed to the double layer, impedance measurements must be made over a wide range of frequencies in order to attain the high frequency limit of the impedance equal to the electrolyte resistance. There are different types of methods used to measure impedance. These include:

2.8.4 Wheatstone bridge:

The AC Wheatstone bridge is one of the oldest methods used to measure the impedance of an electrochemical cell and is only of historical interest now. The typical electrochemical cell generates a potential difference or it needs to have a potential difference impressed upon it to bring it to the condition required by experiment. Therefore the bridge has both an AC and DC detector. Balance of the bridge is indicated by an AC detector which may take the form of a tuned amplifier/meter combination, oscilloscope or some other form of AC voltmeter.

Both R and C have to be balanced simultaneously. This is a slow process, hence the method can be used for only static or slowly varying systems. The arrangement yields the series equivalent of the total cell impedance which includes several impedances such as that of the working electrode, the counter electrode

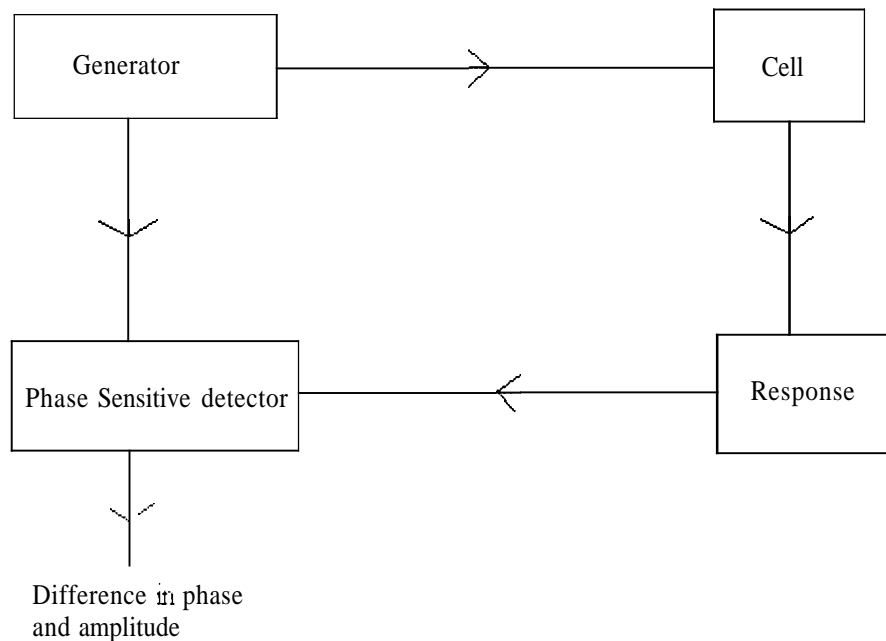
and the resistance of the electrolyte separating them. The main disadvantage of bridge circuits is that it is not possible to make dynamic measurements. They also have a restricted frequency range and cannot be used below about 10 Hz.



A.C. Bridge used for measurement of the impedance of electrochemical cell

2.8.5 Phase sensitive detection:

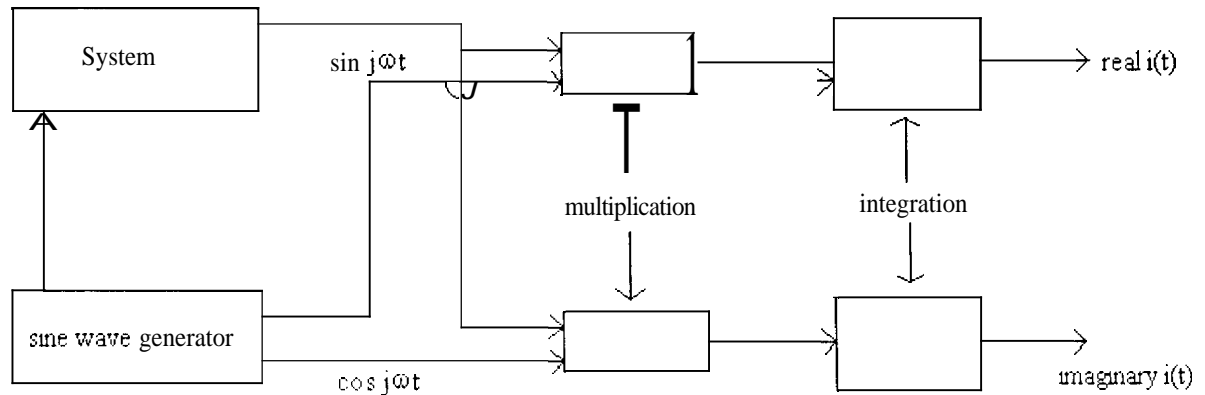
We have used the method of phase sensitive detection by lock-in amplifier [5] to measure the impedance of the electrochemical cell. The potential of the working electrode is held at the desired potential of interest using a potentiostat. A small amplitude sinusoidal voltage input is applied to the cell from a lock-in amplifier. The current output from the cell has a phase difference with respect to the input voltage. The lock in amplifier measures this phase difference and amplitude of the current response.



Principle of functioning of a phase sensitive detector

2.8.6 Frequency response analyser:

The digital frequency response analyser is based on the principle of sine wave correlation [5,7]. The process of sine wave correlation can be described as the multiplication of the measured signal with the sine wave reference derived from the exciting signal. The resulting signal is then integrated over a whole number of cycles of the reference wave, to give a response that is unaffected by harmonics of the reference frequency. Moreover the random noise components are reduced in proportion to the length of the integration period. In practice two reference signals are used which are in phase and in quadrature with the excited signal. The correlator outputs are then proportional to the real part and imaginary part of the admittance.



Schematic of a sine wave correlator showing the process of multiplication of the system output $i(t)$ with reference signals in phase and in quadrature with the exciting signal

2.9 Scanning Tunneling Microscopy:

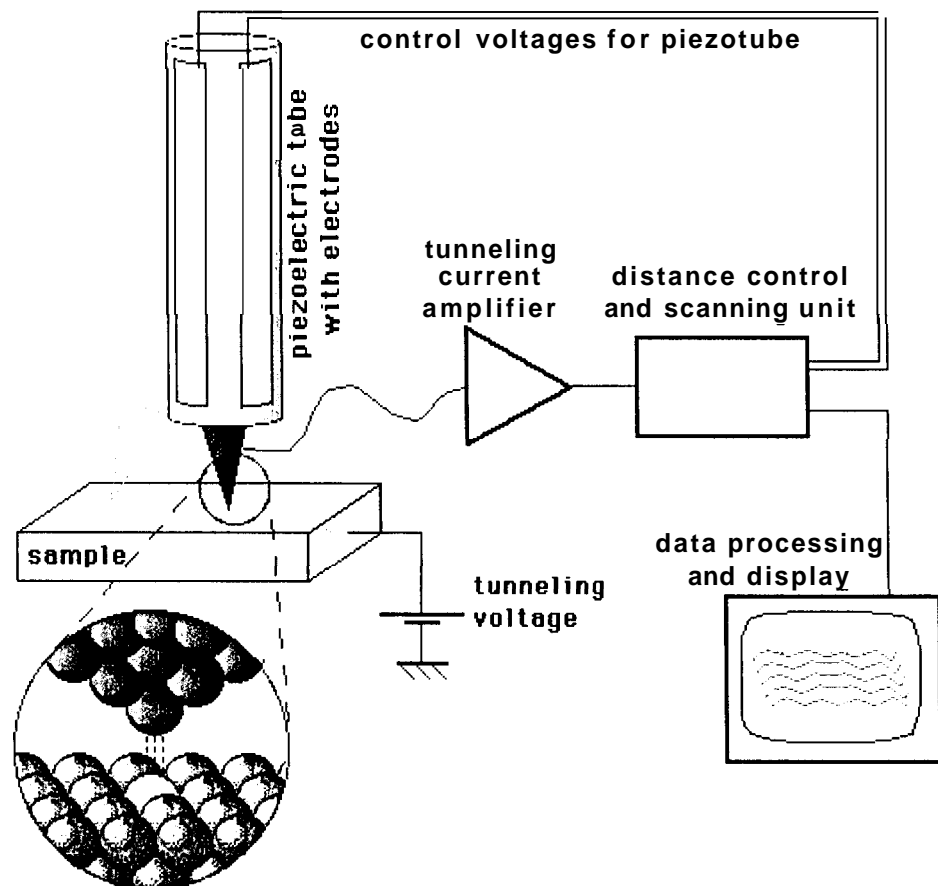
The scanning tunneling microscope (STM)[9] is an excellent device to obtain topographic images of smooth conductive surfaces. It can be used in the investigation of very small areas of surfaces with extremely high level of precision. In a typical STM experiment an atomically sharp metallic tip (Pt/Rh, Pt/Ir, W) is brought very close to the surface (few \AA). The movement of the tip in all the three directions is carried out with the help of piezoelectric crystals. Application of a small potential difference (-1V) between the surface and the tip, leads to the flow of tunneling current. This tunneling is due to the fact that the electron wave functions of the tip and sample overlap. The tunneling current is of the form $I, \approx Ve^{-Cd}$ where I , is the tunneling current, V is the bias voltage, C is a constant that includes the work function of the material and d is the spacing

between the lowest atom on the tip and the highest atom on the sample. The strong exponential dependence of the tunneling current on the tip-to-sample spacing makes it possible to use this current in a feedback loop controlling a precision motion device; i.e. a piezoelectric scanner. In response to an applied voltage, the scanner moves the tip over an area of the sample in a raster pattern and the feedback loop causes the tip to track the sample surface with sub-angstrom precision. The coordinates of the tip's path can then be transformed into a map of the surface topography. Since this current decreases about one order of magnitude per 1 \AA of the electrical gap width, an accuracy of the order of 0.1 \AA can be achieved. This extreme sensitivity of the STM means that features which are of atomic dimensions can be accurately imaged provided the gap distance is accurately controlled. In fact, the STM image at atomic resolution actually corresponds to a contour map of the local density of states (LDOS).

There are two ways to carry out an STM experiment, the first being the constant current and the second the constant height approach. In the first mode the tip is moved slowly in the $y - z$ direction parallel to the sample surface and simultaneously the distance x from the sample surface is adjusted in such a way that the tunneling current is constant. In this mode the tip traces contours of constant electronic densities of the substrate; so a plot of x as a function of y and z gives a topographic image of the electrode surface. In this way the structure of single crystal surfaces, the occurrence of steps, kinks and defects can be seen. In the second mode the tip is moved at a constant height x , while the current is recorded as a function of lateral coordinates. This technique is generally used on atomically smooth substrates only, since on rougher surfaces the tip may hit a protrusion leading to tip crash. In our work we have used a home made STM [10] and the following section describes the features of this STM.

2.9.1 Design of STM:

The major factors in the design of STM involve efficient vibration isolation, minimum thermal drift, proper feedback control, atomically sharp tunneling tips and coarse positioning. Vibration isolation is generally achieved by increasing the resonance frequency of the scan unit such as using tube piezo scanners. The thermal drift is compensated by careful selection of materials and a symmetric design of the scan unit. Very sharp tips can be obtained by electrochemically etched inert metal wires such as Pt- Rh or W. Coarse positioning has been carried



Schematic diagram of Scanning Tunneling Microscope

out using the inertial sliding mechanism. In the inertial sliding arrangement the stage is placed in a position such that when a suitable waveform is applied, the stage moves relative to its starting position by a small increment. This is because the large acceleration provides enough inertial forces that exceed static friction during the falling portion of the saw tooth waveform, while during the slow rise of the waveform the stage essentially follows the piezo motion.

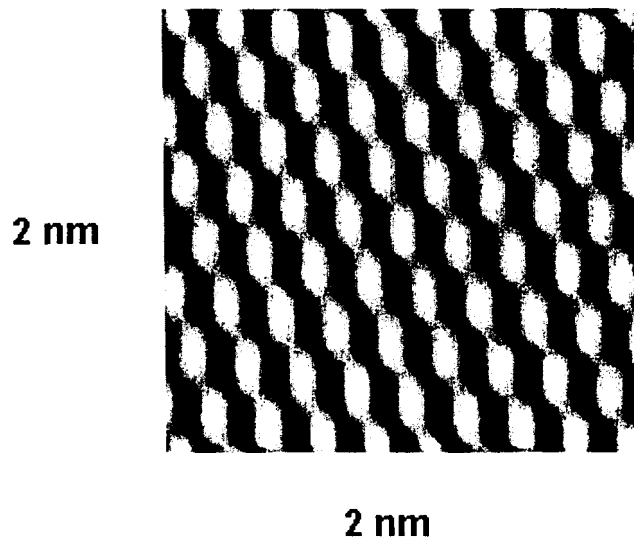
The STM is built of two concentric piezo electric tubes, the inner one for scanning the tip and the outer one for moving the sample holder towards or away from the tip. The piezo tubes have silver metallised coating both on the inside and outside. The inner piezo tube holds the tip wire coaxially. The coarse positioning is achieved by applying a saw tooth voltage to the outer piezo tube whose inside metallised portion is grounded. This compresses the tube resulting in the glass tube containing the sample holder being brought close to the tip. During the sudden release of the tube, during the falling portion of the saw tooth waveform, the glass tube which is attached to the piezo quickly retracts while the sample holder cannot due to inertia. This results in the sample holder being translated towards the tunneling probe by one step. By application of a train of saw tooth pulses of about 120V amplitude and fast scan rate, speeds of the order of 1mm/s both towards and away from the tip are achieved.

The rigidity of the scan unit is one of the important factors in the vibration isolation of the system. The scan unit is mounted inside a nylon block with a hole and is secured by means of two screws to a cylindrical PVC block. The entire assembly, screwed onto a thick brass plate is mounted onto a stack of three more brass plates each separated by a viton O-ring. The whole assembly is suspended using bungee chords to the ceiling.

The STM can be operated either in constant height or constant current mode. In the former mode the tip is scanned over the sample in the same plane, resulting in the variation of the tip-sample separation, which in turn changes the tunneling current. In the constant current mode of operation the tip is scanned such

that the gap separation is always maintained constant at a reference value, by applying a feedback voltage to the inner piezo. The feedback voltage needed for maintaining the tunneling current constant is a measure of the surface topographical changes. The electronics essentially comprises of the current amplifier, analog feedback system, data acquisition using A/D and the piezo drivers comprising of the D/A card interfaced to a PC and high voltage amplifiers.

The feedback unit essentially compares the actual tunneling current with a user specified reference current. If the measured tunneling current is too large, the feedback control system generates a voltage which is applied to the tube scanner to pull the tip back and vice versa. The piezo tube expands linearly with the applied voltage which is in fact directly proportional to the changes in the vertical tip position.



2 nm x 2 nm atomic resolution image of Highly oriented pyrolytic graphite obtained using the STM built in the laboratory.

A personal computer interfaced with a Keithley 500A measurement and control system containing a 16 channel, 16 bit A/D card and two 2 channel 16 bit D/A cards is used for data acquisition and control. The feedback signal from the integrator is fed to one of the channels of the A/D. The current amplifier output representing the tunneling current and the logarithmic amplifier output which provides the logarithm of the tunneling current are fed to another two channels of the A/D respectively. The tip scan and data acquisition proceed concurrently and synchronously. The STM line scan image is displayed in real time. The 3-D images and the density plots are displayed using IDL 5.0 software package. The roughness measurements are carried out using scanning probe image processor (SPIP) programme developed by the Danish Institute of Fundamental Metrology.

REFERENCES

1. H.Silman,G.Isserlis, A.F.Averill *Protective and decorative coatings for metals* Finishing Publications Ltd. 1978.
2. M.Levlin, A.Laakso, H.E.-M.Niemi, P.Hautojarvi *Applied Surface Science* 115 (1997) 31-38.
3. Y.Golan, L.Margulis, I.Rubinstein *Surface Science* 264 (1992) 312-326.
4. A.J.Bard and L.R.Faulkner *Electrochemical Methods – fundamentals and applications*, Wiley New York (1980).
5. *Instrumental methods in Electrochemistry*. Southampton Electrochemistry Group. Ellis Horwood Limited (1990).
6. S.Trasatti, O.A.Petrij *Pure Appl. Chem.* 63 (1991) 711-734.
7. C.Gabrielli *Identification of Electrochemical processes by Frequency response analysis*. Technical Report Number 004183. Schlumberger Solartron Electronic group Ltd.
8. B.D.Cahan, C.T.Chen *J.Electrochem. Soc.* 129 (1982) 700.
9. C.Julian Chen *Introduction to scanning tunneling microscopy*. Oxford University Press (1993).
10. V.Lakshminarayanan *Current Science* 74 (1998) 413-417.